Identification of an unusual variant peroxisome biogenesis disorder caused by mutations in the PEX16 gene

Ebberink, M.S.; Csanyi, B.; Chong, W.K.; Denis, S.; Sharp, P.; Mooijer, P.A.W.; Dekker, C.J.M.; Spooner, C.; Ngu, L.H.; de Sousa, C.; Wanders, R.J.A.; Fietz, M.J.; Clayton, P.T.; Waterham, H.R.; Ferdinandusse, S.

Published in:
Journal of Medical Genetics

DOI:
10.1136/jmg.2009.074302

Identification of an unusual variant peroxisome biogenesis disorder caused by mutations in the *PEX16* gene

Merel S Ebberink,[1] Barbara Csanyi,[2] Wui K Chong,[3] Simone Denis,[1] Peter Sharp,[4] Petra A W Mooijer,[1] Conny J M Dekker,[1] Claire Spooner,[5] Lock H Ngu,[6] Carlos De Sousa,[7] Ronald J A Wanders,[1] Michael J Fietz,[4] Peter T Clayton,[2] Hans R Waterham,[1] Sacha Ferdinandusse[1]

► Additional materials are published online only. To view these files please visit the journal online (http://jmg.bmj.com).

[1]Academic Medical Centre, University of Amsterdam, Laboratory Genetic Metabolic Diseases, Department of Paediatrics/Emma Children's Hospital, Amsterdam, The Netherlands
[2]Biochemistry Research Group, UCL Institute of Child Health, Great Ormond Street Hospital for Children NHS Trust, London, UK
[3]Department of Radiology, Great Ormond Street Hospital for Children NHS Trust, London, UK
[4]National Referral Laboratory, SA Pathology, North Adelaide, Australia
[5]Starship Children's Hospital, Auckland District Health Board, Auckland, New Zealand
[6]Genetics Department, Kuala Lumpur Hospital, Kuala Lumpur, Malaysia
[7]Department of Neurology, Great Ormond Street Hospital for Children NHS Trust, London, UK

Correspondence to
Sacha Ferdinandusse, Laboratory Genetic Metabolic Diseases (F0-220), Academic Medical Centre, University of Amsterdam, Meibergdreef 9, 1105 AZ Amsterdam, The Netherlands;
s.ferdinandusse@amc.uva.nl

Received 19 October 2009
Revised 19 March 2010
Accepted 6 April 2010
Published Online First 20 July 2010

ABSTRACT

Background Zellweger syndrome spectrum disorders are caused by mutations in any of at least 12 different *PEX* genes. This includes *PEX16*, which encodes an integral peroxisomal membrane protein involved in peroxisomal membrane assembly. PEX16-defective patients have been reported to have a severe clinical presentation. Fibroblasts from these patients displayed a defect in the import of peroxisomal matrix and membrane proteins, resulting in a total absence of peroxisomal remnants.

Objective To report on six patients with an unexpected mild variant peroxisome biogenesis disorder due to mutations in the *PEX16* gene. Patients presented in the preschool years with progressive spastic paraparesis and ataxia (with a characteristic pattern of progressive leucodystrophy and brain atrophy on MRI scan) and later developed cataracts and peripheral neuropathy. Surprisingly, their fibroblasts showed enlarged, import-competent peroxisomes.

Results Plasma analysis revealed biochemical abnormalities suggesting a peroxisomal disorder. Biochemical variables in fibroblasts were only mildly abnormal or within the normal range. Immunofluorescence microscopy revealed the presence of import-competent peroxisomes, which were increased in size but reduced in number. Subsequent sequencing of all known *PEX* genes revealed five novel apparent homozygous mutations in the *PEX16* gene.

Conclusions An unusual variant peroxisome biogenesis disorder caused by mutations in the *PEX16* gene, with a relatively mild clinical phenotype and an unexpected phenotype in fibroblasts, was identified. Although PEX16 is involved in peroxisomal membrane assembly, PEX16 defects can present with enlarged import-competent peroxisomes in fibroblasts. This is important for future diagnostics of patients with a peroxisomal disorder.

INTRODUCTION

The Zellweger syndrome spectrum (ZSS), including Zellweger syndrome (ZS; MIM 214100), neonatal adrenoleucodystrophy (MIM 202370) and infantile Refsum disease (MIM 266510), comprises a spectrum of severe, often lethal, inherited multisystemic disorders. Variable neurodevelopmental delay, liver disease, retinopathy and perceptive deafness are characteristic of the disorders within the ZSS. ZS is the most severe disorder within this spectrum. Patients with ZS have profound neurological abnormalities and display typical craniofacial dysmorphia.[1] They generally die within the first year of life. Like patients with ZS, those with neonatal adrenoleucodystrophy experience neonatal hypotonia and seizures. They may have progressive white matter disease, and usually die in late infancy.[2] Patients with infantile Refsum disease have no neuronal migration defect, but can develop a progressive white matter defect. Their survival is variable, but most patients survive beyond infancy and some even reach adulthood.[3]

The disorders of the ZSS are characterised by the absence of functional peroxisomes and a generalised loss of peroxisomal functions. Defects in any of at least 12 different peroxins (PEX), encoded by *PEX* genes, have been found to result in a peroxisome biogenesis disorder (PBD; MIM 601539) of the ZSS type. Peroxins are involved in the import of proteins into the peroxisome and/or the biogenesis of these organelles. Different mutations in the same *PEX* gene can lead to different phenotypes within the spectrum. PEX1, PEX2, PEX5, PEX6, PEX10, PEX12, PEX13, PEX14 and PEX26 are involved in the import of peroxisomal matrix proteins. A defect in one of the genes encoding these peroxins results in impaired peroxisomal matrix protein import, but peroxisomal membrane structures (peroxisomal ghosts) are still present. In contrast, fibroblasts with a defect in the genes encoding PEX3, PEX16 or PEX19, which are involved in the peroxisomal membrane protein import, have been shown to have no peroxisomal remnants at all.[4 5]

Human PEX16 is an integral peroxisomal membrane protein with two membrane-spanning domains. So far, only three patients have been reported with a defect in PEX16, all displaying the severe ZS phenotype. Fibroblasts of these patients showed a complete lack of peroxisomes, including membranes, and peroxisomal functions.[4 6] In this paper, we report on six patients, including one sib pair, who all have a defect in PEX16, but who showed enlarged, protein import-competent peroxisomes in their fibroblasts.

PATIENTS AND METHODS

Patients

Patient 1, a girl, was the first child of consanguineous Turkish parents. She was born at term with a normal birth weight and Apgar scores. She had no dysmorphic features and developed normally until

9 months of age. She started with toe walking at 13 months. Her walking remained unsteady with frequent falls. On examination at the age of 3 years, she presented a normal mental status, a bilateral horizontal nystagmus, increased tone in lower limbs, but normal in upper limbs, normal sensation, ataxia, slight dysmetria, a head and bilateral hand tremor, very brisk tendon reflexes at the knees, extensor plantar reflex and sustained bilateral ankle clonus. She showed no cognitive impairment, no organomegaly and no cranial nerve abnormalities. She stopped walking completely at the age of 5 years and ever since has been wheelchair bound. At the age of 10 years she developed dysarthria and dysphagia, and from that time she required full gastrostomy feeding. At the age of 13 years, ophthalmological examination revealed optic atrophy and very mild lens opacities. At the age of 14 years she was admitted to a hospital for constipation and severe neuropathic pain. On examination, she had normal sensory responses to touch, temperature and pain, but decreased vibration sense (absent in the ankles). Neurophysiology studies revealed evidence of a progressive demyelinating motor and sensory neuropathy affecting upper and lower limbs without axonal involvement on electroneuromyography.

By the age of 16 years, she had spasticity in all four limbs and no independent mobility. Her cataracts had become sufficiently dense as to require surgical removal. Repeated electroretinograms revealed normal flash responses, suggesting normal function of the outer retinal receptor layer, whereas the visual evoked potentials showed small and very delayed potentials, suggesting marked impairment of the visual pathways bilaterally. There have never been any concerns about her hearing.

MRI scans were performed at the age of 4, 6 (figure 1A), 15 and 17 years. They showed extensive, diffuse and symmetrical signal abnormalities of myelinated white matter in the form of increased signal on T2-weighted images and near-normal signal on T1-weighted images. These changes initially involved the dorsal brainstem, internal capsules (more severely in the posterior limb) and deep peritrigonal and parietal white matter, and spared the corpus callosum and subcortical U-fibres of white matter. There was no evidence of a malformation of cortical development. Later scans showed extension of disease into the corpus callosum and the subcortical white matter with some reduction in signal of the involved regions of white matter on T1-weighted images, while remaining more severely abnormal on T2-weighted images. There was generalised prominence of the ventricles and sulci in line with reduction in cerebral volume; however, at the same time, more selective atrophy of the corpus callosum and cerebellar vermis was also observed.

Patient 2 is the younger (by 6 years) brother of patient 1, who was born at term with normal birth weight. He started to walk independently at the age of 17 months, despite lower limb spasticity, with an unsteady gait and frequent falls. He ceased independent walking at 25 months of age and was wheelchair bound from the age of 3 years. On examination at the age of 4 years, he had rigidity particularly in his lower limbs, brisk reflexes, progressive upper limb tremor, dysmetria and dysarthria. A neuropathy became apparent from the age of 5 years with increasing difficulty in emptying his bladder and worsening constipation. At the age of 10 years, a demyelinating motor and sensory neuropathy was shown by electroneuromyography and he developed dysaesthesia in his legs. As for his sister, his flash electroretinogram responses were normal, whereas the visual evoked potential responses were delayed and not very well formed. Cataract was demonstrated. Currently, he is 11 years old and his cognition is relatively spared. His MRI findings (figure 1B,C) resembled those of his sister, showing a similar pattern of progressive leucodystrophy and brain atrophy from the age of 3 years.

The case report of patient 3 was published previously.[7]

No detailed clinical information is available for patient 4.

Patient 5, a girl, was born after an uneventful pregnancy and delivery. Her development was normal in the first year of life, and she started walking independently at the age of 14–15 months. At the age of 2 years, she developed an ataxic gait. At the age of 6 years, she had mild cognitive impairment, moderate dysarthria and abnormal eye saccades, but no problems with speech or swallowing. MRI scans revealed widespread white matter changes on a background pattern of global delay in myelin maturation, with symmetrical white matter abnormality of the dorsal brainstem and capsular white matter, sparing of the corpus callosum and appearing more extensive and conspicuous on T2-weighted images than on T1-weighted images. There was reduced cerebellar volume, more severely affecting the vermis. Similar MRI findings were observed in the sister of patient 5 who was 2 years younger.

Patient 6, a girl, is the second child of consanguineous parents of Indian ethnicity. She was born at term with a normal birth weight. Her development was normal during the first year of life. She walked independently at 13 months and spoke a few short phrases at 18 months. After this she was noted to lose previously acquired skills and did not gain new skills. She lost her ability to walk independently at 24 months due to a combination of spasticity and mild ataxia. Her speech and other cognitive functions also deteriorated slowly over time. At the age of 5 years, nystagmus and cataracts in both eyes were observed. In her lower limbs, the muscular tone was increased, reflexes were brisk, clonus was present and plantar reflexes were up-going. She had mild cerebellar signs. She did not have organomegaly. At 6 years, her cerebral white matter was noted to be diffusely hyperintense compared with grey matter on T2-weighted images in nearly all areas, particularly the deep and capsular white matter. The posterior fossa and callosal white matter was isointense with grey matter—that is, relatively spared. At the same time, all except the subcortical white matter was hyperintense compared with grey matter on T1-weighted images (ie, the comparatively normal appearance of myelinated white matter on these images). In addition, there was evidence of more focal atrophy of the cerebellum and corpus callosum. Peripheral nerve velocity studies of the lower limbs suggested demyelination. Currently, at the age of 9, she is able to stand with a supportive frame, communicate in short sentences, and she is able to read and write simple sentences.

Skin fibroblasts of the patients used in this study were sent to the Laboratory Genetic Metabolic Diseases at the Academic Medical Center of the University of Amsterdam for diagnostic purposes, and informed consent was obtained for publication of the data.

Cell culturing

Primary skin fibroblasts were cultured in Dulbecco's modified Eagle's medium with 4.5 g/l glucose, 584 mg/L L-glutamine (BioWhittaker Lonza; Verviers, Belgium) and 25 mM Hepes, or in HAM F-10 medium with L-glutamine and 25 mM Hepes (Gibco Invitrogen; Carlsbad, California, USA), each supplemented with 10% fetal bovine serum (BioWhittaker), 100 U/ml penicillin, 100 μg/ml streptomycin, in a humidified atmosphere of 5% CO_2, at 37°C. Dulbecco's modified Eagle's medium was used for the transfection experiments, and HAM F-10 medium for the biochemical experiments.

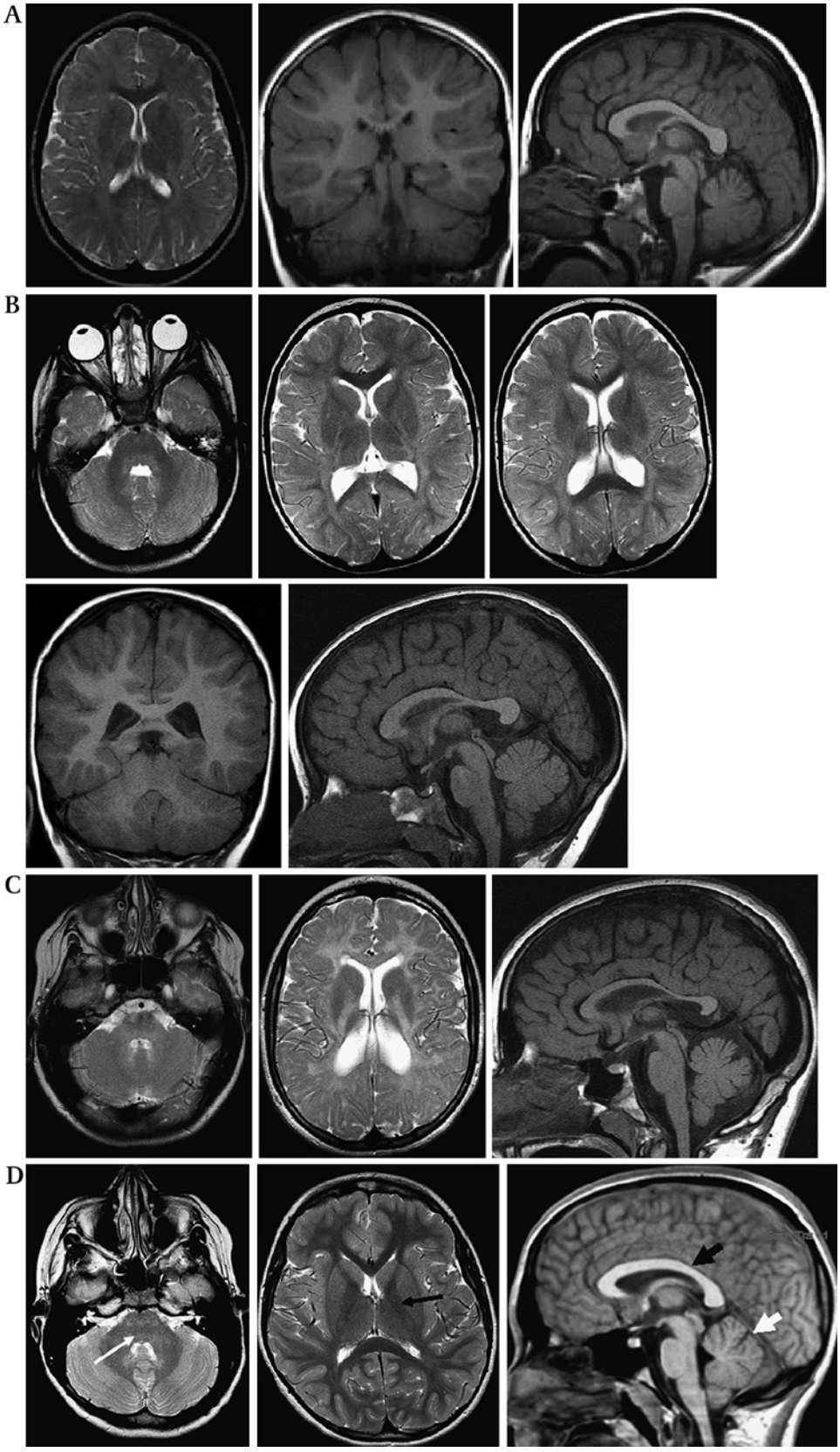

Figure 1 (A) Axial T2-weighted, coronal and sagittal T1-weighted MRI brain images of patient 1 at the age of 6 years. (B) Axial T2-weighted, coronal and sagittal T1-weighted MRI brain images of patient 2 at the age of 3 years. (C) Axial T2-weighted and sagittal T1-weighted MRI brain images of patient 2 at the age of 11 years. (D) Axial T2-weighted and sagittal T1-weighted MRI brain images of a normal child, annotated to show the dorsal brainstem (white arrow), posterior limb of the internal capsule (black arrow), corpus callosum (black arrow head) and cerebellar vermis (white arrow head). All the patient studies showed a pattern of leucodystrophy where the abnormalities were more obvious on the T2-weighted images and less obvious on the T1-weighted images. Atrophy was global but also particularly notable in the corpus callosum and cerebellar vermis.

Biochemical analysis

Levels of very-long-chain fatty acids (VLCFAs), phytanic and pristanic acid, and C_{27}-bile acid intermediates were measured in plasma as described previously.[8] Plasmalogens were determined in erythrocytes as previously described.[9] Dihydroxyacetone phosphate acyltransferase (DHAPAT),[10] acyl-CoA oxidase I (AOXI)[11] and D-bifunctional protein (DBP)[12] activity, concentrations of VLCFAs,[13] β-oxidation of C26:0, C16:0 and pristanic acid,[14] and α-oxidation of phytanic acid[15] were measured in cultured fibroblasts as previously described.

Catalase immunofluorescence and immunoblot analysis using antibodies against peroxisomal thiolase 1, AOXI and DBP were performed as described previously.[12 16]

Mutation analysis

Mutation analysis was performed by either sequencing all exons plus flanking intronic sequences of the *PEX* gene amplified by PCR from genomic DNA or by sequencing cDNAs prepared from total mRNA fractions. Genomic DNA was isolated from skin fibroblasts using the NucleoSpin Tissue genomic DNA purification kit (Macherey-Nagel, Düren, Germany). Total RNA was isolated from skin fibroblasts using Trizol (Invitrogen) extraction, after which cDNA was prepared using a first-strand cDNA synthesis kit for reverse transcription-PCR (Roche, Mannheim, Germany). All forward and reverse primers (*PEX16* primer sequences are listed in online additional table 1) were tagged with a −21M13 (5′-TGTAAAACGACGGCCAGT-3′) sequence or M13rev (5′-CAGGAAACAGCTATGACC-3′) sequence, respectively. PCR fragments were sequenced in two directions using '−21M13' and 'M13rev' primers by means of BigDye Terminator v1.1 Cycle Sequencing Kits (Applied Biosystems, Foster City, California, USA) and analysed on an Applied Biosystems 377A automated DNA sequencer, following the manufacturer's protocol.

Mutation analysis of *PEX1* and *PEX3* was performed by sequencing cDNA. Mutation analysis of PEX2 was performed by sequencing exon 4 from genomic DNA. Mutation analysis of *PEX5L*, *PEX6 PEX10, PEX12, PEX13, PEX14, PEX19* and *PEX26* was performed by sequencing all exons plus flanking intronic sequences.

Mutation analysis of the *PEX16* gene was performed by sequencing the *PEX16* cDNA. Mutations were confirmed by sequencing the corresponding exons and flanking intronic sequences of the *PEX16* gene. Sequences were compared with the reference *PEX16* sequence (NM_004813), with nucleotide numbering starting at the first adenine of the translation initiation codon ATG.

Functional complementation assay

Fibroblasts of the five unrelated patients (2–6) were cotransfected with a pcDNA3 expression plasmid containing either the *PEX16* cDNA (transcription variant 1 containing exon 11a, NM_004813.2) or, as a control, the *PEX12* cDNA (gift from Dr S J Gould), and the pDsRed-Express-DR vector (Clontech Laboratories, Mountain View, CA, USA; used to identify transfected cells) using the Amaxa nucleofector technology (Amaxa, Cologne, Germany). The fibroblasts were examined by catalase immunofluorescence analysis 72 h after transfection.[12] Two independent transfections per construct were examined by counting the number of peroxisomes in at least 100 cells. Similar sized cells with the nucleus in focus were counted under the microscope using a counter.

Expression of mutant *PEX16* cDNA

The mutant *PEX16* cDNAs of patients 1–4 were amplified by PCR from cDNA prepared from mRNA isolated from the patient fibroblasts and subcloned in the mammalian expression vector pcDNA3 (Invitrogen). The wild-type and mutant *PEX16* cDNAs were separately expressed in a previously reported PEX16-deficient fibroblast cell line (homozygous for a p.R298fsX38 mutation) with complete lack of peroxisomal structures[6] and a control fibroblast cell line. Four days after transfection, the fibroblasts were examined by catalase immunofluorescence to assess the appearance of peroxisomes. Two independent transfections per construct were examined by counting the number of peroxisomes in at least 100 cells. Similar sized cells with the nucleus in focus were counted under the microscope using a counter. To control for transfection efficiency, the constructs were also cotransfected with a GFP-SKL expression vector in parallel experiments. The transfection efficiency was comparable for the different constructs.

RESULTS

Biochemical analysis

The major presenting symptom in all cases described for the first time in this paper was difficulty with walking at around 2 years due to a combination of spasticity and ataxia. Presentation with a leucodystrophy at this age has been seen previously in a few children with disorders of peroxisome biogenesis. For this reason, alongside other tests, peroxisomal metabolites were measured in plasma and erythrocytes. The levels of VLCFAs, the branched-chain fatty acids phytanic acid and pristanic acid, and the C_{27}-bile acid intermediates were all raised in plasma (table 1), except for the branched-chain fatty acid levels in patients 1, 5 and 6, which were normal. The levels of plasmalogens in erythrocytes were normal in all patients examined. Studies in cultured skin fibroblasts (table 2) revealed increased levels of VLCFAs with a marginally decreased β-oxidation rate of C26:0 in patients 3–6. All other variables (phytanic acid α-oxidation, pristanic acid β-oxidation and the activity of DHAPAT, the first enzyme of the ether phospholipid biosynthesis pathway) were within the control range. In addition, immunoblot analysis showed that the peroxisomal enzymes AOXI, DBP and thiolase I were normally processed (online additional figure S1). Immunofluorescence microscopy analysis using antibodies raised against catalase, a peroxisomal matrix enzyme, and antibodies against adrenoleucodystrophy (ALD) protein, a peroxisomal membrane protein, revealed the presence of peroxisomes. However, the peroxisomes were markedly enlarged in size and reduced in

Table 1 Biochemical variables in plasma and erythrocytes

			Branched-chain fatty acids		Bile acid intermediates		Plasmalogens (% of total phospholipids)	
	VLCFAs C26/C22 (ratio)	VLCFAs C26:0 (μM)	Phytanic acid (μM)	Pristanic acid (μM)	DHCA (μM)	THCA (μM)	DMA C16:0	DMA C18:0
Control range	0–0.02	0.45–1.32	0–9	0–4	0–0.02	0–0.08	6.8–11.9	10.6–24.9
Patient 1	0.03	2.78	6.8	1.3	n.d.	0.1	10.1	22.7
Patient 2	0.07	4.07	74	24	0.5	0.2	10.5	21.6
Patient 3	0.25	3.00	68	ND	0.2	0.4	ND	ND
Patient 4	0.13	2.83	96	28	4.6	0.95	9.2	20.7
Patient 5	0.03	1.93	10	2	<0.1	<0.1	ND	ND
Patient 6	0.04	2.27	1	1	ND	ND	ND	ND

Plasmalogens were determined in erythrocytes, all other variables in plasma.
VLCFA, very-long-chain fatty acid; DHCA, dihydroxycholestanoic acid; THCA, trihydroxycholestanoic acid; DMA, dimethylacetal; ND, not determined; n.d., not detectable.

Table 2 Biochemical variables in cultured skin fibroblasts

	VLCFAs C26/C22 (ratio)	VLCFAs C26:0 (μmol/g protein)	β-Oxidation (pmol/h/mg protein)		α-Oxidation (phytanic acid; pmol/(h*mg protein)	Enzyme activity		
			C26:0	Pristanic acid		DHAPAT (nmol/(2h*mg protein)	AOXI (pmol/(min*mg protein)	DBP
Control range	0.03–0.07	0.18–0.38	1214–1508	675–1121	39–97	5.8–12.3	92±29	252±79
Patient 2	0.24	0.63	1612	895	69	10.4	72	236
Patient 3	0.29	1.11	930	1317	55	14.2	122	270
Patient 4	0.12	0.62	981	739	64	8.1	71	267
Patient 5	0.12	0.39	916	1058	111	8.6	ND	ND
Patient 6	0.15	0.48	581	832	65	6.6	ND	ND

VLCFA, very-long-chain fatty acid; DHAPAT, dihydroxyacetone phosphate acyltransferase; AOXI, acyl-CoA oxidase I; DBP, D-bifunctional protein; ND, not determined.

number compared with control fibroblasts (figure 2). The presence of enlarged peroxisomes and normal immunoblot profiles, in combination with normal plasmalogen levels and DHAPAT activity usually points to a single peroxisomal enzyme deficiency (ie, AOXI or DBP deficiency). However, measurement of the activities of AOXI and DBP in the patient cells revealed no abnormalities (table 2). On the basis of these results, a novel variant of a PBD with enlarged peroxisomes was suspected.

Mutation analysis

To determine whether the patients had a novel variant of a PBD due to mutations in any of the currently known 12 *PEX* genes, we sequenced all 12 *PEX* genes in either genomic DNA or cDNA prepared from the corresponding mRNAs. Unexpectedly, we identified five novel apparent homozygous mutations in the *PEX16* cDNAs (table 3). The mutations were also checked and appeared homozygous in genomic DNA. The *PEX16* gene is localised at chromosome 11p12–p11.2 and consists of 11 exons. In humans, two different mRNA variants of PEX16 are produced as a result of alternative splicing, each with an alternative exon 11 (exon 11a and exon 11b). Both transcription variants are expressed in human fibroblasts, of which variant 1 containing exon 11a is most abundant. We identified two missense mutations, two small deletions and a large genomic deletion of exon 11a, which are all located at the C-terminus of PEX16. The c.984delG in exon 11a in patients 1 and 2 results in a frameshift and introduces a termination codon at amino acid position 357. Exon 11b is unaffected in patients 1 and 2. The small deletion in patient 3 results in a deletion of a valine at position 252. Patients 4 and 5 both have a missense mutation, leading to the substitution of a threonine for a proline at position 289 (patient 4) and of a cysteine for a tyrosine at position 331 (patient 5), respectively. The c.992A→G (p.Y331C) mutation in patient 5 is located in exon 11a. Patient 6 has a large intragenic deletion in transcription variant 1 comprising the last 468 base pairs of intron 10, the entire exon 11a and the first 80 base pairs of the 3′ flanking region of exon 11a and in transcription variant 2 comprising the last 603 base pairs of intron 10, and the first 4 base pairs of exon 11b. Investigation of the effect of this deletion on cDNA revealed three splice products encoding the following amino acid sequences: p.R318SfsX138, p.R318IfsX38 and p.E296DfsX33.

Complementation assays

To confirm that the identified mutations in *PEX16* are the underlying cause of the peroxisomal abnormalities observed in fibroblasts of the patients, the cell lines were transfected with wild-type *PEX16* cDNA, and *PEX12* cDNA as a negative control. Expression of wild-type *PEX16* cDNA in the cell lines of the unrelated patients (2–6) restored the number of peroxisomes to the number found in control fibroblasts and also reduced the size of peroxisomes to normal (figure 3C). In contrast, expression of wild-type *PEX12* cDNA did not complement the peroxisomal abnormalities in the patient cell lines (figure 3D).

In addition, a fibroblast cell line with a complete PEX16 deficiency, resulting in the total absence of peroxisomal structures, was transfected with wild-type *PEX16* cDNA and the mutant *PEX16* cDNAs of patients 1–4. Expression of wild-type *PEX16* cDNA resulted in more than 100–150 normal sized peroxisomes in nearly all (120 of the 130) transfected cells (figure 3E). However, expression of the *PEX16* cDNAs containing the c.865C→A, c.984delG or c.753_755delTGT mutation resulted in 30–70 enlarged peroxisomes in ~30% of the transfected cells, whereas in the remaining 70% of the transfected cells no restoration of peroxisomes was found.

DISCUSSION

In this study, we identified six patients, including one sib pair, with different defects in PEX16 and an unexpected phenotype in skin fibroblasts. PEX16 was previously shown to be involved in peroxisomal membrane protein import, and, in line with this role, no peroxisomal remnants and a complete lack of peroxisomal functions were found in fibroblasts of the three PEX16-deficient patients reported in the literature to date.[4 6]

Despite the extensive diagnostic work-up in patients 1–4, no definite diagnosis could be made for a long time because the phenotypic presentation was highly unusual for a PBD. The biochemical variables in plasma of these patients showed raised levels of VLCFAs, phytanic acid, pristanic acid and the C_{27}-bile acid intermediates, but normal plasmalogen levels in erythrocytes. Moreover, in fibroblasts, catalase and adrenoleucodystrophy protein (ALDP) immunofluorescence revealed enlarged, import-competent peroxisomes which were reduced in number (figure 2). This phenotype is typical of peroxisomal single enzyme deficiencies—that is, AOXI, but especially DBP, deficiency. However, AOXI and DBP activities were completely normal in these patients. Instead, a defect in PEX16 was identified (table 3).

The identification of the PEX16 defect in patients 1–4 allowed a rapid diagnosis for patients 5 and 6. The fibroblasts of patients 5 and 6 were only recently sent to our laboratory for diagnostic work-up. Because the results of the biochemical tests on their fibroblasts were very similar to the results obtained for patients 1–4, we suspected a possible defect in PEX16. Subsequent mutation analysis indeed revealed mutations in the *PEX16* gene of these patients. This shows that the biochemical phenotype in fibroblasts is consistent. The biochemical presentation in plasma is also similar for all patients examined, although there is some variability in the level of abnormality for both branched-chain fatty acids and bile acid intermediates.

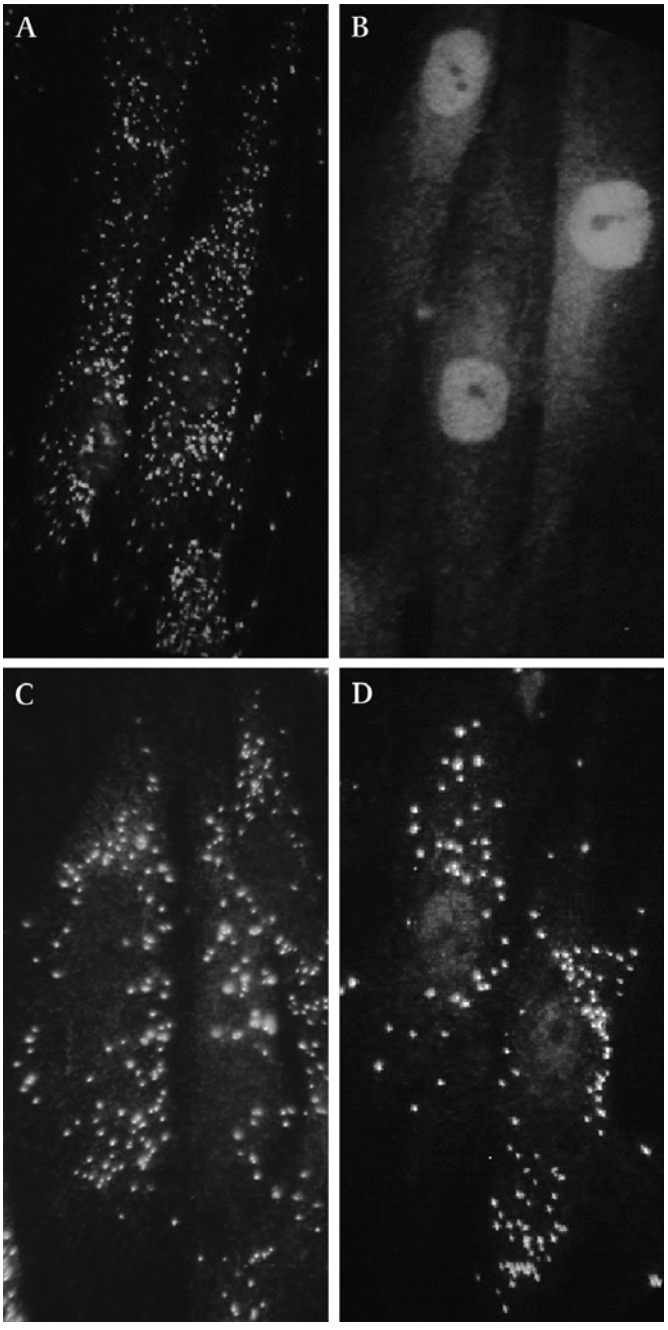

Figure 2 Catalase immunofluorescence in fibroblasts of a control subject (A), a patient with classical Zellweger syndrome (B), a patient with peroxisomal acyl-CoA oxidase I deficiency (C), and patient 3 (D). The phenotype observed in patient 3 with a reduced number of enlarged import-competent peroxisomes was similar to that observed in all five patients examined.

PEX16 contains two transmembrane domains, consisting of amino acids 110–144 and amino acids 222–243. Both the N-terminus and C-terminus are exposed into the cytosol.[17] Amino acids 59–219 are needed for binding to PEX19 and for sorting to the peroxisomal membrane.[18] The mutations that we identified, two missense mutations and three deletions, appear to have a mild effect on the function of PEX16 and are not located in one of the known functional domains of PEX16, but are all located in the C-terminus of PEX16. The detected changes have not been reported previously as either mutations or polymorphisms in the NCBI SNP database. To demonstrate that the mutations we identified cause the phenotype observed in fibroblasts of these patients, we transfected the patient cell lines with wild-type *PEX16* cDNA (transcript variant 1) and studied whether complementation occurred. In addition, the effect of the mutated *PEX16* cDNAs of patients 1–4 on peroxisomal size and number was studied. These experiments showed that the mutant PEX16 proteins are functional, but not to the same extent as wild-type PEX16. The expression of wild-type PEX16 restored biogenesis of peroxisomes in nearly all cells, whereas expression of mutant PEX16 cDNAs resulted in peroxisomes in ~30% of the transfected cells. Possibly, the concentration needed to restore the biogenesis of peroxisomes in all cells was not reached when the mutated *PEX16* cDNAs were used for transfection because of reduced stability of the mutant proteins. Interestingly, two transcription variants of PEX16 exist containing either exon 11a or exon 11b. Three homozygous mutations were identified in exon 11, of which two only affected transcript variant 1 with exon 11a (patients 1, 2 and 5) and one affected both transcript variants (patient 6). The phenotype in fibroblasts was indistinguishable for these different mutations, showing that mutations in transcript variant 1 cause the phenotype of enlarged import-competent peroxisomes. The phenotype of a small number of enlarged peroxisomes caused by the identified mutations in the *PEX16* gene suggests that PEX16 is involved in the morphology and division of peroxisomes in addition to its involvement in membrane assembly.

The peroxisomes in the patients' fibroblasts are able to import matrix and membrane proteins, and this import is sufficient to keep the α- and β-oxidation rate normal (table 2). However, it could very well be that, in other organs such as the liver, peroxisomal functions are more severely affected, since the patients did accumulate peroxisomal metabolites in plasma. This hypothesis is supported by studies in a liver biopsy specimen from patient 3, which showed parenchymal cells with peroxisomes devoid of the matrix enzymes catalase and alanine–glyoxylate aminotransferase.[7]

The observed MRI appearances of progressive leucodystrophy and selective brain atrophy merits some discussion. MR signal characteristics of abnormalities that are greater on T2-weighted than T1-weighted images have previously been described as a 'hypomyelination' pattern of leucodystrophy[19]; however, these changes were seen developing in white matter that had previously appeared normally myelinated on MRI. The observation of selective atrophy of the corpus callosum and cerebellum in combination with this pattern of progressive leucodystrophy is judged to be unique.

In summary, our results show that, in cases with only very mild biochemical peroxisomal abnormalities in fibroblasts, a PBD should not be excluded when peroxisomal metabolites in plasma are abnormal. Moreover, although PEX16 is involved in peroxisomal membrane assembly, PEX16 defects can present with

Table 3 *PEX16* mutations identified

	Mutations		
	Nucleotide	Amino acid	Exon
Patient 1+2	c.984delG	p.I330SfsX27	11
Patient 3	c.753_755delTGT	p.V252del	8
Patient 4	c.865C→A	p.P289T	9
Patient 5	c.992A→G	p.Y331C	11
Patient 6	c.952+118_1011+80	p.R318SfsX138, p.R318IfsX38, p.E296DfsX33	11

Reference sequence of *PEX16*: GenBank accession number NM_004813.2. Nucleotide numbering starts at the adenine of the translation initiation codon ATG.

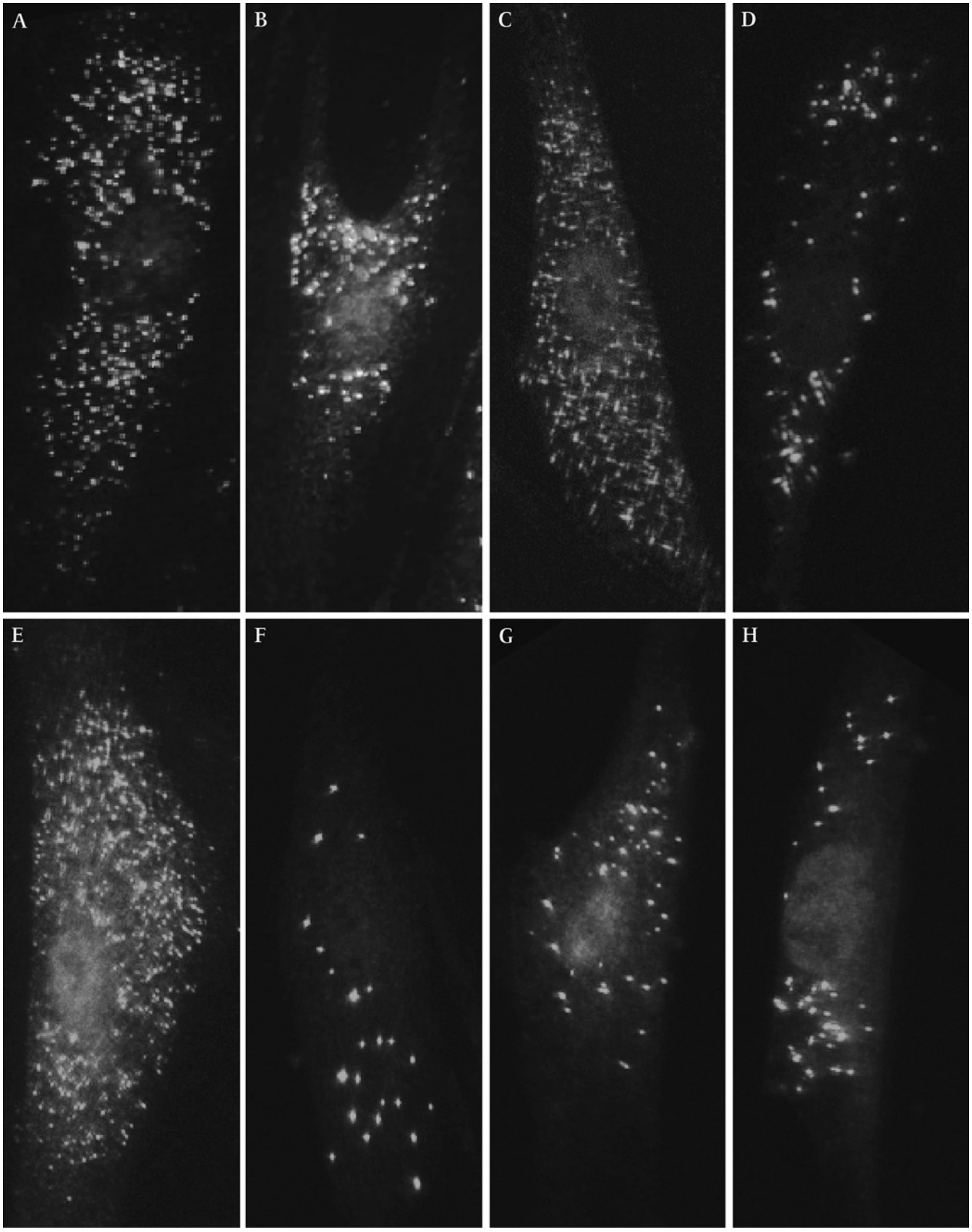

Figure 3 Catalase immunofluorescence in a control cell line (A), patient cell line 4 (B) and patient cell line 4 transfected with *PEX16* cDNA (C) and *PEX12* cDNA (D). Expression of wild-type *PEX16* cDNA resulted in restoration of number and size of peroxisomes in the different patient cell lines. Three mutated *PEX16* cDNA constructs harbouring the mutations identified in patients 1—4 (PEX16_753delTGT (F), PEX16_865C→A (G) and PEX16_984delG (H) were expressed in a complete PEX16-deficient cell line and compared with expression of wild-type *PEX16* cDNA (E). Restoration of peroxisomes was visualised by catalase immunofluorescence 4 days after transfection. Expression of wild-type *PEX16* cDNA revealed full restoration of peroxisome formation in more than 95% of the transfected cells. Expression of the mutated *PEX16* cDNAs revealed 30—70 enlarged peroxisomes in ~30% of the transfected cells.

import-competent peroxisomes in fibroblasts. This is important for future diagnostics of patients with a peroxisomal disorder.

Acknowledgements This study was supported by a grant from the 'Prinses Beatrix Fonds' (MAR 03_0216), the FP6 European Union Project 'peroxisomes' (LSHG-CT-2004512018) and a grant from the Netherlands Organisation for Scientific research (NWO grant 916.46.109). We thank Dr M Pineda and Dr M Giros for referring their patients to us, and we thank the families for their permission to publish this article.

Competing interests None.

Patient consent Obtained.

Provenance and peer review Not commissioned; externally peer reviewed.

REFERENCES

1. **Gould SJ,** Raymond GV, Valle D. *The peroxisome biogenesis disorders*. In: Scriver CR, Beaudet AL, Sly WS, Valle D, eds. *The metabolic and molecular bases of inherited disease*. New York: McGraw-Hill, Inc. 2001:p.2287—324.
2. **Wanders RJ,** Waterham HR. Peroxisomal disorders I: biochemistry and genetics of peroxisome biogenesis disorders. *Clin Genet* 2005;**672**:107—33.
3. **Poll-The BT,** Saudubray JM, Ogier HA, *et al*. Infantile Refsum disease: an inherited peroxisomal disorder. Comparison with Zellweger syndrome and neonatal adrenoleukodystrophy. *Eur J Pediatr* 1987;**1465**:477—83.
4. **Honsho M,** Tamura S, Shimozawa N, *et al*. Mutation in PEX16 is causal in the peroxisome-deficient Zellweger syndrome of complementation group D. *Am J Hum Genet* 1998;**636**:1622—30.
5. **Shimozawa N,** Suzuki Y, Zhang Z, *et al*. Identification of PEX3 as the gene mutated in a Zellweger syndrome patient lacking peroxisomal remnant structures. *Hum Mol Genet* 2000;**913**:1995—9.
6. **Shimozawa N,** Nagase T, Takemoto Y, *et al*. A novel aberrant splicing mutation of the PEX16 gene in two patients with Zellweger syndrome. *Biochem Biophys Res Commun* 2002;**2921**:109—12.
7. **Pineda M,** Giros M, Roels F, *et al*. Diagnosis and follow-up of a case of peroxisomal disorder with peroxisomal mosaicism. *J Child Neurol* 1999;**147**:434—9.
8. **Dacremont G,** Cocquyt G, Vincent G. Measurement of very long-chain fatty acids, phytanic and pristanic acid in plasma and cultured fibroblasts by gas chromatography. *J Inherit Metab Dis* 1995;**18**(Suppl 1):76—83.
9. **Dacremont G,** Vincent G. Assay of plasmalogens and polyunsaturated fatty acids (PUFA) in erythrocytes and fibroblasts. *J Inherit Metab Dis* 1995;**18**(Suppl 1):84—9.
10. **Ofman R,** Wanders RJ. Purification of peroxisomal acyl-CoA: dihydroxyacetonephosphate acyltransferase from human placenta. *Biochim Biophys Acta* 1994;**12061**:27—34.
11. **Wanders BJ,** Denis SW, Dacremont G. Studies on the substrate specificity of the inducible and non-inducible acyl-CoA oxidases from rat kidney peroxisomes. *J Biochem* 1993;**1135**:577—82.
12. **van Grunsven EG,** van Berkel E, Mooijer PA, *et al*. Peroxisomal bifunctional protein deficiency revisited: resolution of its true enzymatic and molecular basis. *Am J Hum Genet* 1999;**641**:99—107.
13. **Vreken P,** van Lint AE, Bootsma AH, *et al*. Rapid stable isotope dilution analysis of very-long-chain fatty acids, pristanic acid and phytanic acid using gas chromatography-electron impact mass spectrometry. *J Chromatogr B Biomed Sci Appl* 1998;**7132**:281—7.
14. **Wanders RJ,** Denis S, Ruiter JP, *et al*. Measurement of peroxisomal fatty acid beta-oxidation in cultured human skin fibroblasts. *J Inherit Metab Dis* 1995;**18**(Suppl 1):113—24.
15. **Wanders RJ,** van Roermund CW. Studies on phytanic acid alpha-oxidation in rat liver and cultured human skin fibroblasts. *Biochim Biophys Acta* 1993;**11673**:345—50.
16. **Wanders RJ,** Dekker C, Ofman R, *et al*. Immunoblot analysis of peroxisomal proteins in liver and fibroblasts from patients. *J Inherit Metab Dis* 1995;**18**(Suppl 1):101—12.
17. **South ST,** Gould SJ. Peroxisome synthesis in the absence of preexisting peroxisomes. *J Cell Biol* 1999;**1442**:255—66.
18. **Fransen M,** Wylin T, Brees C, *et al*. Human pex19p binds peroxisomal integral membrane proteins at regions distinct from their sorting sequences. *Mol Cell Biol* 2001;**2113**:4413—24.
19. **Schiffmann R,** van der Knaap MS. Invited article: an MRI-based approach to the diagnosis of white matter disorders. *Neurology* 2009;**728**:750—9.

Identification of an unusual variant peroxisome biogenesis disorder caused by mutations in the *PEX16* gene

Merel S Ebberink, Barbara Csanyi, Wui K Chong, et al.

J Med Genet 2010 47: 608-615 originally published online July 20, 2010
doi: 10.1136/jmg.2009.074302